Journal of Cellular Physiology

Thermosensitive hybrid hyaluronan/ p(HPMAm-lac)-PEG hydrogels enhance cartilage regeneration in a mouse model of osteoarthritis

Journal:	*Journal of Cellular Physiology*
Manuscript ID	JCP-19-0365.R1
Wiley - Manuscript type:	Original Research Article
Date Submitted by the Author:	16-Mar-2019
Complete List of Authors:	Agas, Dimitrios; Universita degli Studi di Camerino, School of Biosciences and Biotechnology Laus, Fulvio; University of Camerino, School of Biosciences and Veterinary Medicine Lacava, Giovanna; Universita degli Studi di Camerino, School of Biosciences and Biotechnology Marchegiani, Andrea; University of Camerino, School of Biosciences and Veterinary Medicine Deng, Siyuan; Universita degli Studi di Camerino Magnoni, Federico; Universita degli Studi di Camerino Gusmão Silva, Guilherme; Universidade Federal de Minas Gerais DiMartino, Piera; University of Camerino, School of Pharmacy Sabbieti, Maria Giovanna; Universita degli Studi di Camerino, School of Biosciences and Veterinary Medicine Censi, Roberta; University of Camerino, Camerino, School of Pharmacy
Key Words:	osteoarthritis, hyaluronic acid, thermosensitive hydrogels, controlled release

Thermosensitive hybrid hyaluronan/ p(HPMAm-lac)-PEG hydrogels enhance cartilage regeneration in a mouse model of osteoarthritis

Dimitrios Agas[1], Fulvio Laus[2], Giovanna Lacava[1], Andrea Marchegiani[2], Siyuan Deng[3], Federico Magnoni[3], Guilherme Gusmão Silva[1,4], Piera Di Martino[3], Maria Giovanna Sabbieti[1§], Roberta Censi[3§]

[1] School of Biosciences and Veterinary Medicine, University of Camerino Via Gentile III da Varano - 62032 Camerino (MC), Italy

[2] School of Biosciences and Veterinary Medicine, University of Camerino, Via Circonvallazione 93/95 - 62024 Matelica (MC), Italy

[3] School of Pharmacy, University of Camerino, Via. S. Agostino, 1 - 62032 Camerino (MC), Italy

[4] Departamento de Bioquímica e Imunologia, Universidade Federal de Minas Gerais, Belo Horizonte, Minas Gerais, Brazil

§ The authors equally contributed to this work

Corresponding authors: Dimitrios Agas, School of Biosciences and Veterinary Medicine, University of Camerino, Via Gentile III da Varano, I-62032 Camerino (MC) Italy; Tel. +39-737-402713/15; e-mail: dimitrios.agas@unicam.it

Maria Giovanna Sabbieti, School of Biosciences and Veterinary Medicine, University of Camerino, Via Gentile III da Varano, I-62032 Camerino (MC) Italy; Tel. +39-737-402715; e-mail: giovanna.sabbieti@unicam.it

Author contribution statement

G.L., S.D., F.M. performed the experiments, R.C., D.A, M.G.S., P.DM. designed the experiments, analysed the data, and wrote the manuscript, G.G.S., A.M. performed the statistical analysis, F.L., A.M. performed and supervised the animal treatments, P.D.M. and M.G.S. provided the financial support to the study.

Running Head: Hybrid hyaluronan/ p(HPMAm-lac)-PEG hydrogels in cartilage regeneration

Keywords: osteoarthritis, hyaluronic acid, thermosensitive hydrogels, controlled release, degradation.

Total number of figures: 6

Funding statement: This project was supported by the EU research grant H2020-MSCA-ITN- 2015 number 675743, by the EU research grant H2020-MSCA-RISE-2016 number 734684, by an H2020-MSCA-RISE-2017 award through the CANCER project (grant number 777682) and by FAR Unicam research grant number BVI000014.

Conflict of interest statement

The authors declare that the research was conducted in the absence of any commercial or financial relationships that could be construed as a potential conflict of interest

ABSTRACT

Osteoarthritis, due to cartilage degeneration, is one of the leading causes of disability worldwide. Currently, there are not efficacious therapies to reverse cartilage degeneration. In this study we evaluated the potential of hybrid hydrogels, composed of a biodegradable and thermosensitive triblock copolymer cross-linked via Michael addition to thiolated hyaluronic acid, in contrasting inflammatory processes underlying osteoarthritis. Hydrogels composed of different w/w % concentrations of hyaluronan were investigated for their degradation behavior and capacity to release the polysaccharide in a sustained fashion. It was found that hyaluronic acid was controllably released during network degradation with a zero-order release kinetics, and the release rate depended on cross-link density and degradation kinetics of the hydrogels. When locally administered in vivo in an osteoarthritis mouse model, the hydrogels demonstrated ability to restore, to some extent, bone remineralization, proteoglygan production, levels of Sox-9 and Runx-2. Furthermore, the downregulation

of pro-inflammatory mediators, such as TNF-α, NFkB, and RANKL and pro-inflammatory cytokines was observed. In summary, the investigated hydrogel technology represents an ideal candidate for the potential encapsulation and release of drugs relevant in the field of osteoarthritis. In this context, the hydrogel matrix could act in synergy with the drug, in reversing phenomena of inflammation, cartilage disruption and bone demineralization associated with osteoarthritis.

INTRODUCTION

Osteoarthritis (OA) is a progressive, degenerative joint disease that affects, only in the US, over 30 million people over 50 years of age, involving not only the elderly, but also young and active individuals with prolonged participation in physical-demanding activities (Zhang and Jordan, 2010). OA is characterized by the damage or breakdown of articular cartilage and subchondral bone, particularly those of the hands, hips and knees. The transient proliferative response of chondrocytes observed in early OA is progressively suppressed by the increased synthesis of catabolic cytokines and matrix-degrading enzymes in the chronic stage of the disease (Goldring, 2000). The degrading cartilage matrix shows increased water content and lower tensile strength, leading to symptomatic pain, joint stiffness, swelling, and disability for the patients (Sophia Fox et al., 2009). Cytological and histological aberrations, typical of inflammatory synovitis, such as synovial lining hyperplasia, infiltration of macrophages and lymphocytes, neoangiogenesis and fibrosis are often associated with OA (Scanzello and Goldring, 2012). From a biochemical point of view, engagement of Toll-like receptors, activation of the complement cascade, and the synthesis and release of a wide variety

of cytokines and chemokines are the expression of the inflammatory processes underlying OA (Scanzello and Goldring, 2012; Sellam and Berenbaum, 2010).

Currently, treatments to halt OA disease progression are not available. Symptomatic treatment of the affection is the only practicable option, with the use of analgesics, non-steroidal anti-inflammatory drugs, corticosteroids being the most commonly applied therapies. However, these pharmacological approaches did not prove long-term efficacy and and they have all been associated with adverse effects (Bellamy et al., 2006; Raynauld et al., 2003). At the end stage of the disease, arthroplasty is usually needed (McAlindon et al., 2014). Recently, new strategies, such as anti-cytokine therapy, gene therapy, delivery of growth factors, stem-cell therapy, and new lubricant agents, such as lubricin, have been proposed (Chevalier et al., 2010). Viscosupplementation of hyaluronic acid (HA) is used to augment the viscoelastic properties of OA synovial fluid, which has been shown to have a lower concentration and molecular weight of HA compared to healthy fluid (Moreland, 2003). The hyaluronan in normal synovial fluid plays an important role in joint homeostasis. It contributes to joint lubrication, buffers load transmission across articular surfaces, provides a renewed source of hyaluronan to joint tissues, and imparts anti-nociceptive and anti-inflammatory properties to synovial fluid (Marshall, 2000). There are currently several commercially available hyaluronate or hyaluronate derived viscosupplementation agents composed of native sodium hyaluronate (e.i. Hyalgan®, Sanofi-Synthelabo Inc., New York, NY), or chemically cross-linked hyaluronic acid (e.i. Hylan G-F 20, Synvisc®, Wyeth-Ayerst, Philadelphia, PA). The residence time of HA upon intraarticular injection is relatively short for the non-crosslinked polymer (24 hours), while the chemically cross-linked HA resided in the synovium for over 28 days. However, the degradation kinetics of such polysaccharides are poorly controllable, as

mainly mediated by phagocytosis (Jackson and Simon, 2006). The scope of the present work was to investigate the anti-inflammatory effect in an osteoarthritic mouse model of low molecular weight HA, that was chemically cross-linked to and controllably release from a new hydrogel system, via a mechanism mediated by hydrolysis rather than cellular metabolism. Hydrogels are water swollen three-dimensional polymer networks that hold potential in the field of cartilage regeneration, as they can act both as scaffolding materials and/or releasing matrices for biologically active and cell modulating substances. Their water content, soft nature and porous structure mimic biological tissues and make them suitable to accommodate cells and to encapsulate and release water-soluble compounds like proteins in a controlled fashion (Censi et al., 2012).

The hydrogel used in the present work was previously designed (Dubbini et al., 2015) and appropriately optimized in the present work for the application in osteoarthritis management. The administration strategy is minimally invasive, as the system is thermos-responsive, therefore undergoes phase transition at body temperature, generating a hydrogel depot at the site of injection. Furthermore, the system is fully degradable via a mechanism that mainly depends on polymer hydrolysis (Censi et al., 2010).

In our previous studies, we showed the design and synthesis of a new hyaluronic acid/PEG-p(HPMAm-lac)-based hydrogel and demonstrated its potential as cell and protein carrier. Also, we tested its biocompatibility in vitro and in vivo (Sabbieti et al., 2017). In the present study, we investigated its efficacy in osteoarthritic mouse models in reducing articular inflammation by the controlled delivery of HA. This study will pave the way towards the application of the HA-cross-linked hydrogel as delivery system for regenerative molecules for cartilage tissue engineering, such as anti RANKL

antibodies. The local administration of such drugs may potentially minimize side effects compared to intravenous administration, that usually requires large doses because of its poor localization to diseased joints.

MATERIAL AND METHODS

Materials

Unless indicated otherwise, all the chemicals were obtained from Sigma-Aldrich and used as received. Sodium hyaluronate with a molecular weight of 37900 Da was supplied by LIFECORE BIOMEDICAL. Hydroxypropyl methacrylamide mono- and di-lactate (HPMAm-lac$_1$ and HPMAm-lac$_2$) were synthesized according to a previously reported method (Soga et al., 2004). The synthesis of triblock copolymers with PEG as middle block and poly(HPMAm-lac$_{1-2}$) as outer blocks was described previously (Vermonden et al., 2006). 3,3'-Dithiobis(propanoic dihydrazide) (DTP) was synthesized by the method described by Vercruysse et al., 1997.

Methods

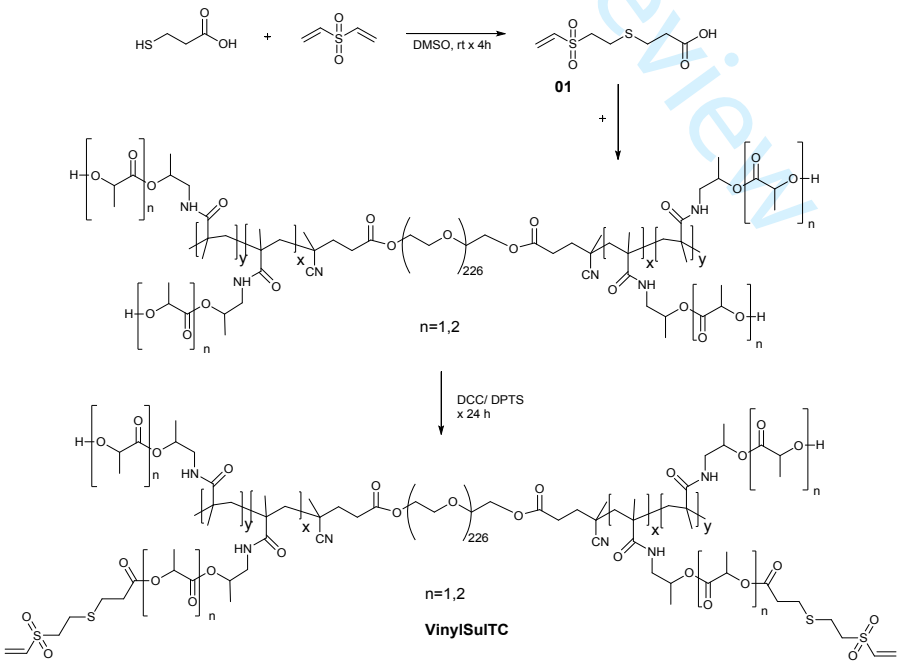

Scheme 1. One-Pot Synthesis procedure for vinyl sulfonated triblock copolymers based on poly(HPMAm-lac$_{1-2}$)-PEG- poly(HPMAm-lac$_{1-2}$)

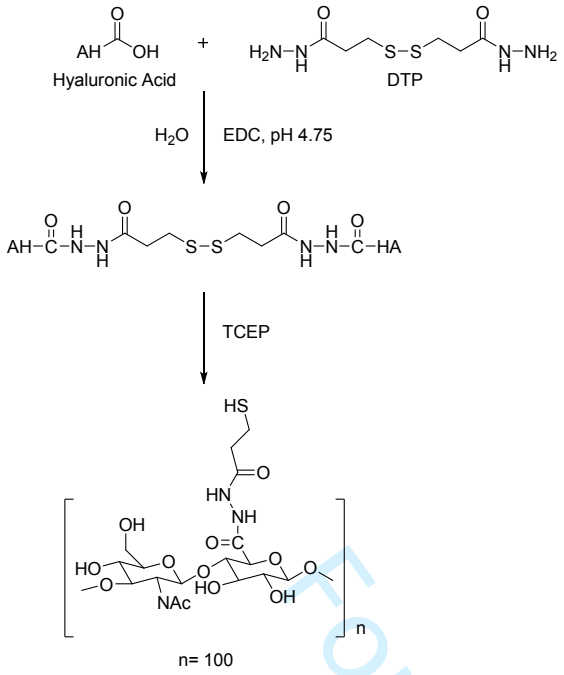

Scheme 2. Synthesis route of thiolated hyaluronic acid

Synthesis of Vinyl Sulfonated triblock copolymer

Triblock copolymers of an aimed degree of substitution (DS) of 0, 10 and 15% were synthesized and indicated as VinylSulTC_0, VinylSulTC_10 and VinylSulTC_15, respectively. The DS is defined as the number of vinyl sulfone groups per lactate residues. As an example, the synthesis procedure of VinylSulTC_10 is reported. Divinyl sulfone (DVS) (0.114 mol) was dissolved in 100 ml dimethyl sulfoxide (DMSO). Subsequently, 3-Mercapto propionic acid (3-MPA) (0.0057 mol), was added dropwise at a molar ratio of 1:20 compared to DVS and the reaction was stirred at room temperature for 4 h. Separately, p(HPMAm-lac)-PEG (0.000221 mol), 4-(Dimethylamino)pyridinium 4-toluensulfonate (DPTS) (0.00085 mol, molar ratio of DPTS to 3-MPA of 0.15:1), N,N'-Dicyclohexylcarbodiimide (DCC) (0.0085 mol, molar ratio of DCC to 3-MPA is 1.5:1) were dissolved in DMSO (10 ml per gram of triblock copolymer) and added dropwise to the previous mixture at a molar ratio between free hydroxyl groups of p(HPMAm-lac)-PEG and 3-MPA of 1:0.20 and

reacted for 24 h at room temperature. The vinyl sulfone modified triblock copolymer p(HPMAm-lac)-PEG was purified by dialysis for 48 h at 4°C against water (MWCO 12-14 KDa) and freeze-dried (Hiemstra et al., 2007; Dubbini et al., 2015). The synthesized product was characterized by ^{1}H-NMR, GPC and light scattering. The DS was determined by ^{1}H-NMR and calculated from the ratio of the intensity of the peaks at 6.3-6.2 and 6.9 and intensity of the peak at 5.4-5.2 ppm according to the equation: $(I_{6.3\text{-}6.2} + I_{6.9} / 3) / (I_{6.3\text{-}6.2} + I_{6.9} / 3 + I_{5.4\text{-}5.2})$ x 100.

Before Vinyl sulfonation. ^{1}H-NMR, $CDCl_3$, δ in ppm: 6.9 (1H, -N*H*CH_2CHCH_3), 5.0 (2H, -NHCH$_2$C*H*(CH_3)O and -COC*H*(CH_3)O), 4.4 (1H, -COC*H*(CH_3)OH), 3.8-3.4 (909 H, -OC*H*$_2$C*H*$_2$ PEG protons), 3.1 (2H, -NHC*H*$_2$), 2.2-0.8 (main chain protons).

After Vinyl sulfonation. ^{1}H-NMR, DMSO-d_6, δ in ppm: 7.3 (1H, -N*H*CH_2CHCH_3), 6.9 (1H, -SO$_2$C*H*=CH$_2$), 6.3-6.2 (2H, -SO$_2$CH=C*H*$_2$), 5.4-5.2 (1H, -O*H*$CHCH_3$), 4.9-4.8 (2H, -NHCH$_2$C*H*(CH_3)O and -COC*H*(CH_3)O), 4.2-4.1 (1H, -COC*H*(CH_3)OH), 3.5 (909 H, -OC*H*$_2$C*H*$_2$ PEG protons), 2.7 (8H, -C*H*$_2$C*H*$_2$SC*H*$_2$C*H*$_2$) 1.7-0.7 (main chain protons).

Synthesis of Thiolated Hyaluronic Acid (HA-SH)

Thiolated hyaluronic acid was synthesized slightly modifying the procedure described by Shu et al., (2002). One gram of sodium hyaluronate (Mn 37.9kDa) was dissolved in 100 ml of sterile water and 482 mg of 3-3'-dithiobis propanoic diidrazide (DTP) was added while stirring. The pH was adjusted to 4.75 with HCl 2 M and, subsequently, 388 mg of 1-ethyl-3-[3-(dimethylamino)propyl]-carbodiimide (EDC) was added while keeping the pH at 4.75. The solution was stirred at room temperature for 48 h and the reaction was stopped by increasing the pH to pH 7 with NaOH 5 M. Then, 1.5 g of Tris(2-carboxyethyl)phosphine hydrochloride (TCEP) was added as reducing agent.

The reaction mixture was stirred for additional 24 h. The mixture was purified by dialysis (MWCO 12-14 kDa) against dilute HCl (pH 3.5) containing 100mM NaCl and finally against water at 4 °C. The final product was obtained as a white powder after lyophilization (Censi et al., 2010). The degree of substitution (DS), defined as the number of DTP residues per 100 disaccharide units, was determined by ^{1}H-NMR and Ellman's method (Riener et al., 2012). The products obtained is indicated as HA-SH_56.

^{1}H- NMR, D_2O, δ in ppm: 4.6-3.2 protons of hyaluronic acid, 2.7 (CH_2SH), 2.5 (CH_2CH_2SH), 1.8 ($NHCOCH_3$).

^{1}H-NMR Spectroscopy

NMR spectra were recorded with a Varian Mercury Plus 400 NMR spectrometer. The polymers were dissolved in $CDCl_3$, DMSO-d_6 and D_2O. Chemical shifts were referred to the solvent peak.

Gel Permeation Chromatography (GPC)

The weight average molecular weight (Mw), the number average molecular weight (Mn) and the Polydispersity Index (PDI) of the vinyl sulfonated triblock copolymer were determined by gel permeation chromatography (GPC) using a TSKgel G4000HHR column (TOSOH BIOSCIENCE), 7.8 mm ID x 30.0 cm L, pore size 5 µm. PEGs of defined molecular weights, ranging from 106 to 1015000 Da) were used as calibration standards. The eluent was THF, the elution rate was 1.0 ml/min and the temperature of the column was 35°C. The samples were dissolved in THF at a concentration of 5 mg/ml.

Cloud point (CP)

The cloud point of the polymer was determined using a Zetasizer Nano-S90 of Malvern Instruments. The temperature gradient range between 5°C to 40°C, 1°C/min. The samples are dissolved in Ammonium Acetate buffer 120 mM pH 5.0 with the concentration of 3-5 mg/ml.

Hydrogel formulation

For in vitro testing, hydrogels of a volume of 100 µL were prepared in cylindrically shaped glass vials (diameter of 5 mm) as follows. VinylSulfTC_10 or VinylSulfTC_15 were dissolved in phosphate buffer at pH 7.4 for at least 2 hours at 4 °C. HA-SH_56 was separately dissolved in phosphate buffer pH 7.4 at room temperature and gently mixed to the previously prepared triblock copolymer solutions. Upon mixing, the hydrogels were incubated at 37°C for 1 hour to allow thermal gelation and subsequent Michael addition cross-linking. The final concentration of VinylSulfTC_10 or VinylSulfTC_15 was 15% w/w, while the HA-SH_56 solid content was calculated in order to have a vinyl sulfones/thiol groups molar ratio of 1/1, resulting in 4.1 and 8.2% w/w for VinylSulTC_10 and VinylSulTC_15 based hydrogels, respectively.

Hydrogels used for *in vivo* studies were formulated using the same procedure described above but sterile saline was used as solvent. The two polymer solutions were mixed immediately upon injection and tanden thermal and chemical cross-linking occurred *in vivo*, at the inoculation site. As a control, physical hydrogels composed of VinylSulfTC_0 dissolved in sterile saline at 15% w/w concentration were applied *in vivo*.

Rheology

Rheological characterization was performed on a Physica – MCR 101 (Anton Paar) rheometer equipped with a Peltier plate and a 20 mm 1° steel cone-plate geometry. A layer of silicone oil of viscosity of 0.05 Pa.s was wrapped around the edge of the conical geometry to prevent water evaporation. A temperature sweep test from 18 to 37°C at a heating rate of 1°C/min was performed at a frequency of 1Hz and 1% strain were used.

Swelling and degradation test

Hydrogels, prepared as described in the previous section, were supplemented with 900 µL of saline phosphate buffered (PBS pH 7.4, 150 mM) and allowed to swell. The swollen hydrogels were weighted at regular time intervals after removing the exceeding buffer. Subsequently the buffer was refreshed. The swelling ratio of the hydrogels was calculated from the initial hydrogel weight after preparation (W_0) and the swollen hydrogel weight after exposure to buffer (W_t):

Swelling Ratio (SR) = W_t / W_0

HA release studies

Gels were prepared as described above and surmounted with 0.9 mL of PBS buffer pH 7.4. The vials were incubated at 37°C under gentle horizontal shaking. Next, 0.15 mL of solution was withdrawn at regular intervals and replaced by an equal amount of fresh buffer. The release of HA from the formulated hydrogels was determined by using an Aure A base glycosaminoglycan colorimetric assay. Ten µl aliquots of the release media were combined with 190 µl of 0.025 mg/ml Azure A in a 96-well plate. The absorbance at 620 nm was measured on an Infinite 200 PRO, Tecan Spectrophotometer. The concentration of HA in the solution was determined from an experimentally-obtained calibration curve.

Animal studies

All the protocol and procedures employed (experimental animals and housing and husbandry) were ethically reviewed and approved by the Italian Ministry of Health, authorization n° 933/2016-PR, conforming to the Directive 2010/63/EU.

Animals and Treatments

Balb/c male mice (Harlan SrL, San Pietro al Natisone Udine, Italy) weighing between 25 - 30 g were selected. Mice were kept in laminar-flow cage in standardized environmental conditions. Food and water were supplied ad libitum.

Mice (7-9 weeks old) were randomized in three groups (G1: control group; G2: experimental groups) and they were anesthetized by administration of 4% isoflurane (induction) followed by 2% isoflurane (maintenance) in combination with a 2:1 mixture of O2/N2O. Then, mice were intra-articularly injected in the left knee with only in sterile physiological saline (G1, *n: 6*) or with collagenase from *Clostridium histolyticum* (10 μg) using a 26-gauge (26 G) needle (G2, *n: 30)* (van der Kraan et al., 1990).

One week following collagenase administration, the two groups of mice were anesthetized with isoflurane-air mixture to perform X-ray analysis (as better described below) to confirm that the treatment with collagenase was able to induce osteoarthritis. Then, the G2 group was further divided in five subgroups and, after receiving anesthesia, they were intradermal injected close to hind limb knee joint as below detailed: G2b (*n = 6)* was administered with 50 μl of only physiological saline; G2c (*n = 6*) was administered with 50 μl control physically crosslinked hydrogel composed of 15% w/w VinylSulfTC_0 in saline and in the absence of hyaluronic acid (no HA); G2d,

(*n* = *6*) was administered with 50 µl chemically crosslinked hydrogel composed of 15% w/w VinylSulfTC_10 at a DS of 8% and 4.1% w/w thiolated hyaluronic acid at a DS of 56% in saline (HA 1x). G2e (*n* = *6*) was administered with 50 µl chemically crosslinked hydrogel composed of 15% w/w VinylSulfTC_15 at a DS of 16% and 8.2% w/w thiolated hyaluronic acid at a DS of 56% in saline (HA2x).

The group G2a did not received any further treatment. Also, since the effects of the VinylSulfTC_10/HA-SH_56 hydrogel on healthy mice were previously reported (Sabbieti et al., 2017), the G1 control group did not receive any further treatment; by this way we avoid the unnecessary use of animals. Table 2 gives an overview of the experimental plan for *in vivo* studies.

Three weeks after the treatments, anesthetized mice were subjected to X-ray analysis (as better described below) and, immediately prior to be sacrificed, the anesthetized mice underwent blood samples collection, by cardiac puncture, to measure the level of seric cytokines. Then, all animals were sacrificed by CO_2 narcosis under the supervision of authorized investigators. Anesthesia, X-ray and euthanasia were performed by accredited veterinarian physician involved in these studies.

ROI and quantitative X-ray analysis

Anesthetized mice were positioned in dorsal recumbence, as previously described (Agas et al., 2017), making sure that pelvis, femurs and tibias were included in radiographs. A portable X-ray generator (Gierth HF 80/15 plus ULTRA LEICH, Gierth X-Ray International GmbH, Germany) mounted on a stative with focal distance of 60 cm was used; X-ray applied dose was 54Kv for a time of 0,04 sec. Radiographs were acquired in DICOM format with Fujifilm FCR Capsule X (Fujifilm Corporation, Japan) and processed both with Osirix (Pixmeo SARL, Switzerland) and ImageJ

(http://rsb.info.nih.gov/ij/) software, according to image analysis protocols previously reported (McManus and Grill, 2011; Waung et al., 2014). Bone mineral density (BMD) was evaluated on the knee joint by OsiriX software. The areas selected were defined as the region of interest (ROI).

Subsequently, the DICOM images were converted with ImageJ into TIFF images and a 16 intervals pseudo-color scale was applied to the color scale. This scale starts from black pixels (value of zero) and increased gradations of mineralization density are represented in 16 equal intervals by a pseudo-color scheme to white pixels (value of 255). Hence, distribution of pixels in the same ROI, defined as above described, was calculated and displayed as an histogram.

Histological analysis

Hind-limbs were dissected at the hip and fixed in 4% paraformaldehyde (PFA) diluted in PBS for 72 h at 4°C 4%. Then, bones were decalcified in 14% ethylenediaminetetraacetic acid (EDTA) solution (pH 7.1) at RT for 3 days under constant agitation. Samples, after dehydration, were embedded with paraffin. Tissue sections, 10-12 μm thick, were obtained by a microtome (Leica Reichert-Jung 2040). Sections were stained with Safranin-O/fast green and graded for cartilage defect healing using a cartilage scoring previously described (Glasson et al., 2007). Briefly, each knee yielded 13e16 slides for scoring by two blinded observers using a modified semi-quantitative grading scale 8, where 0 represented normal cartilage; 0.5: loss of Safranin-O with no structural lesions; 1: roughened articular surface and small fibrillations; 2: fibrillation below the superficial layer and some loss of lamina; 3: fibrillations extending to the calcified cartilage across less than 20% of the cartilage width; 5: fibrillation and erosions extending from 20 to 80% of the cartilage width; 6: cartilage erosion extending beyond 80% of the cartilage width. Blinded histological scoring was

performed on the four quadrants: medial and lateral femoral condyles and medial and lateral tibial plateaus.

Total bone marrow cell (BMCs) and bone marrow stromal cell (BMSCs) preparation and cultures

Long bones (femurs, tibiae and humeri) from the above mice groups (not used for the histological analysis) were dissected free of adhering tissues. Epiphyses were removed and the marrow cavity was flushed. Total Bone Marrow Cells (BMCs) were cultured for 2 days in DMEM plus 10% heat-inactivated-fetal calf serum (HIFCS), penicillin, and streptomycin (Invitrogen, Milano, Italy). Then, culture medium and cells were collected to study the release of cytokines and chemokines and the pro-inflammatory in the cells lysate, respectively.

Other BMCs cells from the same mice groups were maintained in culture for 10 days in order to generate monolayers of adherent cells (Bianco et al., 2013), referred as Bone Marrow Stromal Cells (BMSCs).

Cytokines and chemokines assay

The cytokine/chemokine profiles in supernatants of 2 days cultured BMCs population as well as in serum samples were assessed by using Mouse Cytokine Array Panel A kit (R&D Systems, Milano, Italy) accordingly to the manufacturer's instructions. Immunoreactive dots were visualized using LiteAblot Turbo luminol reagents (Euroclone, Milano, Italy) and Hyperfilm-ECL film (Euroclone, Milano, Italy) and quantitated densitometrically.

Western blotting

Proteins from total BMCs and from BMSCs were extracted in Cell Lysis Buffer (Cell Signaling Euroclone, Milano, Italy) after 2 days of cultures and the concentration was determined by the BCA protein assay reagent (Pierce, Euroclone Milano, Italy). Western blotting was performed as previously described (Sabbieti et al., 2010). Membranes were immunoblotted in blocking buffer with specific antibodies: rabbit anti-TNFα and rabbit anti-NF-kB (BioLegend, Microtech SrL, Napoli, Italy) both diluted 1:500; mouse anti-RANKL and rabbit anti-Runx-2 (Abcam, Prodotti Gianni, Milano, Italy) all diluted 1:600; rabbit anti-SOX-2 (Santa Cruz Biotechnology, Inc. DBA, Milano, Italy) diluted 1:300. After washing with PBS-T, blots were incubated with horseradish peroxidase (HRP)-conjugated donkey anti-rabbit IgG (Cell Signaling, Euroclone Milano, Italy) both diluted 1:50,000. Immunoreactive bands were visualized using LiteAblot Turbo luminol reagents (Euroclone, Milano, Italy) and Hyperfilm-ECL film (Euroclone, Milano, Italy) accordingly to the manufacturer's instructions. To normalize the bands, filters were stripped and re probed with a monoclonal anti-α-tubulin (Sigma-Aldrich, Milano, Italy). Bands density was quantified densitometrically.

Statistical analysis

All data were expressed as a mean ± standard error (S.E.). Two-way analysis of variance (ANOVA) was used to compare the among the mice groups. Tukey test was used in multiple comparisons among all groups. All the statistical analyses were performed using the GraphPad Prism (v 6.01) on a personal computer O.S. Windows 10. Data were presented as mean ± S.E. Values of $p < 0.05$ were considered significant.

RESULTS & DISCUSSION

Synthesis and *in vitro* characterization of the hydrogel networks

All polymers were successfully synthesized and fully characterized as shown in Table 1 of the previous section. Hydrogels, analyzed for rheological behavior, showed a continuous increase of storage modulus for both hydrogel formulations, with HA2x hydrogels reaching higher values of G' as compared to HA1x hydrogels (**Fig. 1A**). These data were in agreement with literature, reporting higher values of G' for hydrogels of higher cross-link density and higher solid content (Dubbini et al., 2015; Censi et al., 2009). Rheology measurements also demonstrated successful Michael addition cross-linking, that progressed as G' increased. Immediately upon temperature increase, the formulated hydrogels reached their gel-point at the temperatures of 20 and 22 °C for HA1x and HA2x hydrogels, respectively (**Fig. 1B**). Also these findings were in agreement with literature data, demonstrating the dependence of the gel point not only on the cloud of the polymer but also on the initial polymer content (Vermonden et al., 2006).

In order to assess the efficiency of Michael addition cross-linking, after one hour cross-linking at 37 °C, the networks were hydrolyzed in basic conditions and the unreacted vinyl sulfone groups were quantified according to the method previously described by Dubbini et al., (2015). As shown in **Figure 1 C**, the chromatograms of the cross-linked hydrogels showed no detectable peak of free DVS-3MPA, indicating that during the chemical cross-linking reaction, the conversion of α-β unsaturated groups was, within the experimental error, complete.

When placed in contact with physiological buffer at 37 °C, both hydrogel formulations showed hydrolytical biodegradability that led to the observation of two different phenomena. On the one hand, the swelling and weight loss of the polymeric matrix, and, on the other hand, the release of hyaluronic acid. **Figure 2A** shows the swelling ratio of the two hydrogel networks as a function of time of exposition to the physiological conditions. It can be observed how both hydrogels, already from early time-points, demonstrated a certain tendency to absorb water, reaching SR values between 2 and 2.5 after 5 and 10 days for HA2x and HA1x, respectively. Water uptake is due to chain relaxation of the polymers involved in the hydrogel networks and to the hydrolysis of the free lactate groups, that make the network more hydrophilic and prone to water absorption. When the hydrolysis of the cross-links starts, polymer chains solubilize in the medium resulting in weight loss by the network. The complete dissolution of the hydrogel in medium was reached after approximately 40 and 70 days, respectively. As expected, the hydrogels displaying a higher cross-link density and a higher content of HA (HA2x) showed a longer residence time in physiological medium as compared to HA1x, as a higher number of ester bonds needed to hydrolyze before complete dissolution of the network.

After a lag-phase of approximately 7 days, a continuous zero-order release of HA was observed for both hydrogel formulations in a timeframe ranging from approximately 7 to 32 days for HA1x and from 7 to 60 days for HA2x, with tunable release rates according to gel composition (**Fig. 2B**). Particularly, hydrogels of lower cross-link density and lower polymer content (HA1x) displayed a faster release rate as compared to HA2x. Zero-order kinetics are often associated to a degradation-driven release mechanism, indicating that HA is released from the network only after hydrolysis of the cross-links. The faster release of HA from HA1x networks depends on the faster

degradation kinetics of the hydrogel (Censi et al., 2009). The degradation time of the hydrogels corresponded with good agreement to the release time of HA. No burst release of HA was observed, indicating that Michael addition cross-linking occurred *in vitro* to a high extent and no detectable unbound HA existed. HA total recovery ranged between 65 and 70% for both formulations. The reason for the non-quantitative recovery of HA was the possible release of HA as aggregate to small hydrogel fragments that may have been detached from the bulk hydrogel during the pipetting and may have not been quantified by Azure A assay. Figure **2C** shows the cumulative release of HA expressed in absolute amount of polymer as a function of time. As expected, HA1x released a lower amount of HA than HA2x because the initial hydrogel formulations differed for HA content.

In vivo efficacy testing of the hydrogels in osteoarthritis mouse models

The osteoarthritic mouse model was obtained by intra-articular injection of collagenase to anesthetized mice and the validity of the procedure was verified by X-ray analysis one week after the treatment. Collagenase injection induced a notable reduction of bone mineral density (BMD) (**Figure 3A**).

In order to evaluate whether the hyaluronic acid was able to decrease the inflammatory process in osteoarthritic knees, the osteoarthritic mice were divided in five groups: two groups were injected with hydrogel containing two different doses of hyaluronic acid (4.1% and 8.2% as detailed in Materials and Methods section); the remaining three groups, used as controls, were injected with the only saline, with the hydrogel alone or did not received any additional injection. Our previous work evidenced that the main decrease of pro-inflammatory cytokines, induced by hyaluronic acid, was obtained 21 days after intradermal administration in healthy mice of hydrogels composed of HA

and thermosensitive triblock copolymers of poly(HPMAm-lac$_{1-2}$)-PEG-poly(HPMAm-lac$_{1-2}$) (Sabbieti et al., 2017). Also, according to previous observations, the hydrogel degradation *in vivo* was accelerated by the enzymatic activity of hyaluronidases and by cellular metabolism (Sabbiet et al., 2017), therefore it is likely that the release of HA from the hydrogel matrices *in vivo* would be faster that that observed *in vitro*. Hence, 21 days upon the administration of different hydrogel formulations, all mice were anesthetized and subjected to X-ray and cardiac puncture prior to be sacrificed.

A statically significantly increase of BMD was observed in osteoarthritic mice treated with HA1x or HA2x compounds, while no changes in BMD were found in osteoarthritic mice treated with saline or HA0x, indicating that the presence and the release of HA in the hydrogel composition was efficacious in modulating the mineral content of bones. Moreover, the effects of hyaluronic acid effects were dose dependent, as a more evident effect on bone remineralization was observed for HA2x with respect to HA1x (**Fig. 3B**).

Histological evaluation of the articular cartilage showed profound pathological changes in mice injected with collagenase, characterized by loss of chondrocytes and extracellular matrix proteoglycans and glycosaminoglycans (Schmitz et al., 2010) content compared with control (**Fig. 4 A, B**). On the other hand, assessment of the knee joints sections of mice receiving HA1x or HA2x after collagenase injections, showed a partial restoration of the cartilage evidenced by an increase of thickness and cellularity as well as a more homogeneous Safranin-O staining (**Figure 4 E, F**). No significant effects in cartilage repair were found in mice treated with saline or HA0x (**Figure 4 C, D**), supporting the initial hypothesis that the controlled release of HA from jellified matrices would have a positive effect on osteoarthritis.

Also, specific markers of mesenchymal stem cells (MSCs) differentiation in chondroblasts such as Sox-2 and Runx-2 were evaluated in BMSCs from healthy and osteoarthritic mice treated or untreated with hydrogels based on hyaluronic acid. In particular, Sox-9 stimulates the production of the cartilage extracellular matrix components such as type II collagen and aggrecan (Tsuchiya et al., 2003), while Runx-2 regulates chondroblast and osteoblast maturation (Sabbieti et al., 2009).

As shown in **Figure 5 A,** the synthesis of both Sox-9 and Runx-2, that was drastically down-regulated in collagenase-injected mice, was restored only by treatments with HA2x and HA1x.

Previous findings demonstrated that, from a clinical point of view, osteoarthritic patients develop synovitis to a variable extent. It is thought that several cytokines and other mediators, particularly tumor necrosis factor (TNF)-α and interleukin (IL)-1, may play a key role in both synovial inflammation and in the activation of chondrocytes and synovial fibroblasts (Goldring and Goldring, 2007). These cytokines are able to start a vicious cycle of stimulation of their own production, and induce the production of IL-6, IL-8, leukocyte inhibitory factor, proteases and prostaglandins by synovial cells and chondrocytes. It is known that TNFα and IL-1 are key mediators of inflammation and articular cartilage destruction. On these bases, currently investigated therapies rely on the use of anticytokine compounds (Bondeson et al., 2010). In line with these studies, we found an increase of pro-inflammatory markers such as Tumor Necrosis Factor (TNF)-α and nuclear factor kappa-light-chain-enhancer of activated B cells (NFkB) in BMSCs from osteoarthritic mice, accompanied with an up-regulation of the osteoclastogenic master regulator RANKL. Interestingly, the administration of HA1x and HA2x not only diminished these inflammatory molecules but also induced a

decrease of osteoclasts maturation contrasting in this way the risks of bone loss (**Fig. 5B**).

Similarly, the hydrogel-hyaluronic acid compounds reduced the enhanced secretion of pro-inflammatory cytokines/chemokines detected both in total BMCs supernatants and in the serum of collagenase-injected mice (**Fig. 6 A, B**).

The evidences provided in this study support the hypothesis that the controlled release of hyaluronic acid from biocompatible and biodegradable injectable matrices prolongs the exposure of osteoarthritic joints to hyaluronic acid. This compound promotes the resolution of osteoarthritic-related clinical manifestations, by exerting sustained anti-inflammatory effect. The efficacy of hyaluronic acid in osteoarthritis may relie on its selective interactions with CD44+ cells, such as chondrocytes, that overexpress CD44 receptors in the course of osteoarthritis (Dosio et al, 2016; Mero et al., 2014). The primary mechanism of action of hyaluronic acid in the context of OA is the binding with CD44 receptor (Altman et al., 2015). CD44 is a cell-surface glycoprotein expressed in articular cells. Hyaluronic acid binding to CD44 inhibits interleukin (IL)-1β expression, leading to a decline in the production of various matrix metalloproteinase (MMP). This inhibition of MMPs prevents catabolic enzyme activity within the joint cartilage. Furthermore, through the reduction of disintegrins and metalloproteases, HA-CD44 binding decreases chondrocyte apoptotic events. This decrease of chondrocyte apoptosis avoids the production of reactive oxygen species (ROS) within the synovium, such as nitric oxide (NO), that also contributes to cartilage degeneration. Additional events related to CD44-HA binding include reduction of prostaglandin PGE_2 and increased expression of heat shock protein 70. Hyaluronic acid regulates inflammation also via the binding with RHAMM receptors (Misra et al, 2015). It is also demonstrated that hyaluronan also regulates nerve sensitivity and

enhances the synthesis of proteoglycans (Holyoak et al., 2016). Finally, the safety, viscoelasticity and biodegradability (enzymatic degradation by hyaluronidases) of hyaluronan make this viscoelastic material particularly suitable as joint lubricant, preventing cartilage degeneration through decreased friction (Maheu et al., 2016).

The continuous presentation of hyaluronic acid to the osteoarthritic joints via the degradation-mediated release from the hydrogels, sustains over a prolonged period of time the previously described physiological activities of the polysaccharide. This results in a higher efficacy of treatment compared to non-cross-linked hyaluronan, having poor residence time in the joints.

CONCLUSIONS

In conclusion, we showed for the first time that (HPMAm-lac$_{1-2}$)-PEG-p(HPMAm-lac$_{1-2}$)/thiolated hyaluronic acid hydrogels are able to contrast the inflammatory process in a mouse model of osteoarthritis through the controlled and sustained release of hyaluronic acid over a time period that goes from 30 to 70 days *in vitro*. In our previous research performed on healthy mice, we assumed that the observed anti-inflammatory effects of these compounds were attributable to the enrichment of the polymer networks with hyaluronic acid. In this study, we confirmed and demonstrated our hypothesis since the administration of the hydrogels not containing hyaluronic acid was did not contrast osteoarthritis, while hydrogels composed of hyaluronic acid displayed a dose-dependent effect in the reversion of inflammation related symptoms of osteoarthritis. Importantly the developed hybrid hydrogels, not only inhibited the release of inflammatory molecules, but were also able to induce mesenchymal stem cells (MSCs) maturation into chondroblasts and new cartilage formation. Since it is known that the inflammatory environments alter MSCs

differentiation, we postulated that the reduction of inflammatory signals induced by the sustained release of Hyaluronan, reestablished the physiological MSCs behavior. Hence, this research could provide additional insights into potential therapeutic applications of biomaterials and, more importantly, it could suggest the use of hyaluronic acid hydrogels as controlled delivery system for advanced therapies against osteoarthritis.

REFERENCES

Agas D, Gusmão Silva G, Laus F, *et al*. 2017; INF-γ encoding plasmid administration triggers bone loss and disrupts bone marrow microenvironment. *J Endocrinol* **232**:309-21.

Altman RD, Manjoo A, Fierlinger A, *et al*. 2015; The mechanism of action for hyaluronic acid treatment in the osteoarthritic knee: a systematic review. *BMC Musculoskelet Disord* **16**: 015-0775.

Bellamy N, Campbell J, Robinson V, *et al*. 2006; Intraarticular corticosteroid for treatment of osteoarthritis of the knee. *Cochrane Database Syst Rev* **2**: CD005328.

Bianco P, Cao X, Frenette PS, *et al*. 2013; The meaning, the sense and the significance: Translating the science of mesenchymal stem cells into medicine. *Nat Med* **19**: 35-42.

Bondeson J, Blom AB, Wainwright S, *et al*. 2010; The role of synovial macrophages and macrophage-produced mediators in driving inflammatory and destructive responses in osteoarthritis. *Arthritis Rheum* **62**:647-57.

Censi R, Di Martino P, Vermonden T, *et al.* 2012; Hydrogels for protein delivery in tissue engineering. *J Control Rel* **161**: 680-92.

Censi R, Fieten PJ, Di Martino P, *et al*. 2010; In situ forming hydrogels by tandem thermal gelling and Michael addition reaction between thermosensitive triblock copolymers and thiolated hyaluronan. *Macromolecules* **43**:5771-78.

Censi R, Vermonden T, Deschout H, *et al*. 2010; Photopolymerized thermosensitive poly (HPMAlactate)-PEG-based hydrogels: effect of network design on mechanical properties, degradation, and release behavior. *Biomacromolecules* **11**: 2143-51.

Censi R, Vermonden T, van Steenbergen MJ, *et al*. 2009; Photopolymerized thermosensitive hydrogels for tailorable diffusion-controlled protein delivery. *J Control Rel* **140**: 230-6.

Chevalier X. 2010; Intraarticular treatments for osteoarthritis: new perspectives. *Curr Drug Targets* **11**: 546-60.

Dosio F, Arpicco S, Stella B, *et al*. 2016; Hyaluronic acid for anticancer drug and nucleic acid delivery. *Adv Drug Delivery Rev* **97**:204-36.

Dubbini A, Censi R, Butini ME, *et al*. 2015; Injectable hyaluronic acid/PEG-p(HPMAm-lac)-based hydrogels dually cross-linked by thermal gelling and Michael addition. *Europ Pol J* **72**: 423-37.

Glasson SS, Blanchet TJ, Morris EA. 2007; The surgical destabilization of the medial meniscus (DMM) model of osteoarthritis in the 129/SvEv mouse. *Osteoarthritis and Cartilage* **15**:1061-69.

Goldring MB, Goldring SR. 2007; Osteoarthritis. *J Cell Physiol* **213**: 626-34.

Goldring MB. 2000; The role of the chondrocyte in osteoarthritis. *Arthritis & Rheumatism* **43**:1916-26.

Hiemstra C, Zhou W, Zhong Z, *et al*. 2007; Rapidly in situ forming biodegradable robust hydrogels by combining stereocomplexation and photopolymerization. *J Am Chem Soc* **129**: 9918-26.

Holyoak DT, Tian YF, van der Meulen MC, *et al*. 2016; Osteoarthritis: Pathology, Mouse Models, and Nanoparticle Injectable Systems for Targeted Treatment. *Ann Biomed Eng* **44:** 2062-75.

Jackson DW, Simon TM. 2006; Intra-articular distribution and residence time of Hylan A and B: a study in the goat knee. *Osteoarthritis and Cartilage* **14**:1248-57.

Maheu E, Rannou F, Reginster JY. 2016; Efficacy and safety of hyaluronic acid in the management of osteoarthritis: Evidence from real-life setting trials and surveys. *Semin Arthritis Rheum* **45**: 2.

Marshall KW. 2000; Intra-articular hyaluronan therapy. *Curr Opin Rheumatol* **12**: 468-74.

McAlindon TE, Bannuru RR, Sullivan MC, *et al.* 2014; OARSI guidelines for the non-surgical management of knee osteoarthritis. *Osteoarthritis and Cartilage* **22**:363-88.

McManus MM, Grill RJ. 2011; Longitudinal evaluation of mouse hind limb bone loss after spinal cord injury using novel, in vivo, methodology. *J Vis Exp* **7**.

Mero A, Campisi M. 2014; Hyaluronic Acid Bioconjugates for the Delivery of Bioactive Molecules. *Polymers* **6**.

Misra S, Hascall VC, Markwald RR, *et al*. 2015; Interactions between Hyaluronan and Its Receptors (CD44, RHAMM) Regulate the Activities of Inflammation and Cancer. *Front Immunol* **6**.

Moreland LW. 2003; Intra-articular hyaluronan (hyaluronic acid) and hylans for the treatment of osteoarthritis: mechanisms of action. *Arthritis Res & Ther* **5**:54-67.

Raynauld JP, Buckland-Wright C, Ward R, *et al*. 2003; Safety and efficacy of long-term intraarticular steroid injections in osteoarthritis of the knee: A randomized, double-blind, placebo-controlled trial. *Arthritis & Rheumatology* **48**: 370-77.

Riener CK, Kada G, Gruber HJ. 2002; Quick measurement of protein sulfhydryls with Ellman's reagent and with 4,4'-dithiodipyridine. *Anal Bioanal Chem* **373**: 266-76.

Sabbieti MG, Agas D, Marchetti L, *et al*. 2010; Signaling pathways implicated in PGF2alpha effects on Fgf2+/+ and Fgf2-/- osteoblasts. *J Cell Physiol* **224**: 465-74.

Sabbieti MG, Agas D, Xiao L, *et al*. 2009; Endogenous FGF-2 is critically important in PTH anabolic effects on bone. *J Cell Physiol* **219**: 143-51.

Sabbieti MG, Dubbini A, Laus F, *et al*. 2016; In vivo biocompatibility of p(HPMAm-lac)-PEG hydrogels hybridized with hyaluronan. J Tissue Eng Regen Med **11**:3056-3067.

Scanzello CR, Goldring SR. 2012; The role of synovitis in osteoarthritis pathogenesis. *Bone* **51**: 249-57.

Schmitz N, Laverty S. Kraus VB, et al., 2010; Basic methods in histopathology of joint tissues. *Osteoarthritis and Cartilage* **18**: S113eS116.

Sellam J, Berenbaum F. 2010; The role of synovitis in pathophysiology and clinical symptoms of osteoarthritis. *Nat Rev Rheumatol* **6**:625-35.

Shu XZ, Liu Y, Luo Y, *et al*. 2002; Disulfide cross-linked hyaluronan hydrogels. *Biomacromolecules* **3**:1304-11.

Soga O, van Nostrum CF, Hennink WE. 2004; Poly(N-(2-hydroxypropyl) methacrylamide mono/di lactate): a new class of biodegradable polymers with tuneable thermosensitivity. *Biomacromolecules* **5**:818-21.

Sophia Fox AJ, Bedi A, Rodeo SA. 2009; The Basic Science of Articular Cartilage: Structure, Composition, and Function. *Sports Health* **1**:461-68.

Tsuchiya H, Kitoh H, Sugiura F, *et al*. 2003; Chondrogenesis enhanced by overexpression of sox9 gene in mouse bone marrow-derived mesenchymal stem cells. *Biochem Biophys Res Commun* **301**: 338-43.

van der Kraan PM, Vitters EL, van Beuningen HM, *et al*. 1990: Degenerative knee joint lesions in mice after a single intra-articular collagenase injection. A new model of osteoarthritis. *J Exp Pathol* **71**:19-31.

Vercruysse KP, Marecak DM, Marecek JF, *et al*. 1997; Synthesis and in vitro degradation of new polyvalent hydrazide cross-linked hydrogels of hyaluronic acid. *Bioconjug Chem* **8**: 686-94.

Vermonden T, Besseling NAM, van Steenbergen MJ, *et al*. 2006; Rheological Studies of Thermosensitive Triblock Copolymer Hydrogels. *Langmuir* **22**:10180-84.

Waung JA, Maynard SA, Gopal S, *et al*. 2014; Quantitative X-ray microradiography for high-throughput phenotyping of osteoarthritis in mice. *Osteoarthritis and Cartilage* **22**:1396-400.

Zhang Y, Jordan JM. 2010; Epidemiology of Osteoarthritis. *Clinics in geriatric medicine* **26**: 355-69.

FIGURE LEGENDS

Figure 1. Rheology measurements of HA1x and HA2x hydrogels. Storage moduli (G') and loss moduli (G'') as a function of time at increasing temperature (A). Close-up image of rheology experiments, where the gel point is observed at the cross-point of G' and G'' (B). HPLC analysis of unreacted vinyl sulfone groups of HA2x hydrogels after 1 hour Michael addition cross-linking at 37°C. Comparison with standard vinyl sulfone and vinyl sulfone hydrolyzed from uncross-linked hydrogels (C).

Figure 2. Swelling and degradation profiles of HA1x and HA2x hydrogels shown as the variation in time of the SR value during storage of the networks in physiological conditions (exposure to phosphate buffer at pH 7,4 and 37 °C (A). HA release profiles from HA1x and HA2x hydrogels: cumulative release profile % as a function of time (B); cumulative release profile in mg as a function of time (C).

Figure 3. Pseudo-color images of X-ray images obtained converting the original 16 bit DICOM X-ray radiographs to an 8 bit TIFF format and pseudo-coloring the resultant image using a 16 color look-up table. In pseudo-color images, lower bone mineral density (BMD) is represented in green and yellow pseudo-colors, while higher BMD is represented in red and purple pseudo-colors. Histograms represent the BMD calculated in the areas selected (ROI). The decreased BMD after intraarticular injection of collagenase is visualized in green/yellow pseudo-color. The treatment

with HA1A HA2x hydrogel in collagenase-injected mice resore the BMD, (yellow/purple and red/white pseudo-color, respectively) in dose dependent manner (A, B).

Figure 4. Representative Safranin-O/fast green stained histological sections of the knee joints in all mice groups (n = 6 mice/group) (A-F). Arrows indicated areas of hypocellularity after collagenase injection (B). HA1x and HA2x compounds reconstitute the cartilage thickness and cellularity (E, F). Magnification 10x. Cartilage erosion scores for femoral and tibial surfaces. Scores (mean±SE) shown with femoral condyles and tibial plateaus. Each group consisted of 6 animals (G).

Figure 5. Representative western blotting of SOX-9 and RUNX2 expression levels in BMSCs obtained from all the mice groups (A). Representative western blotting of TNF-α, NFkB, and RANKL levels in BMSCs from all the mice groups (B). Data were analyzed by using two-way ANOVA. Lowercase letters denote homogeneous subsets. Error bars represent ± SE ($p < 0.05$)

Figure 6. Cytokines release analyzed in medium from total bone marrow cell (BMCs) cultures (A) and in serum (B) of the all mice groups; Data were analyzed by using two-way ANOVA. Lowercase letters denote homogeneous subsets. Error bars represent ± SE ($p < 0.05$)

Figure 1

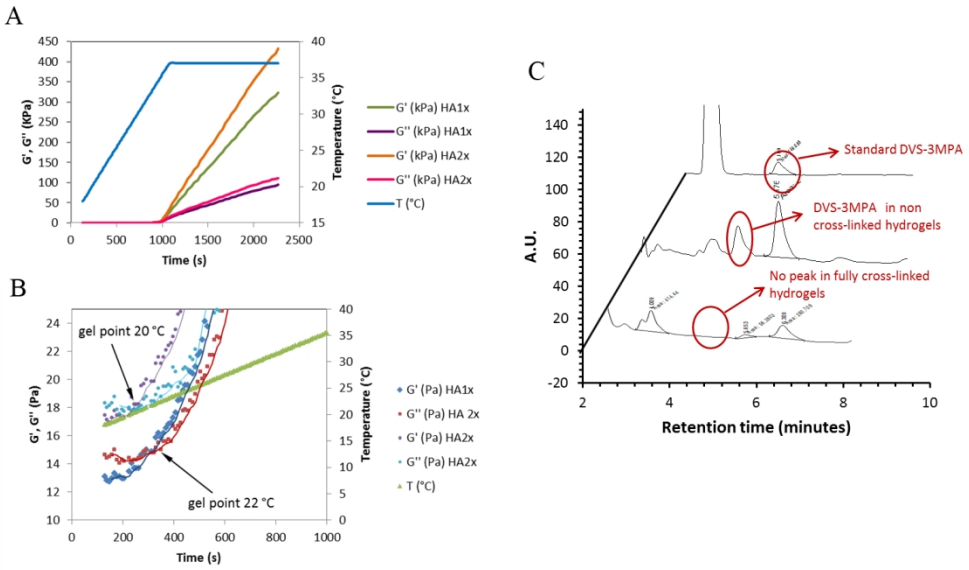

Figure 1. Rheology measurements of HA1x and HA2x hydrogels. Storage moduli (G') and loss moduli (G'') as a function of time at increasing temperature (A). Close-up image of rheology experiments, where the gel point is observed at the cross-point of G' and G'' (B). HPLC analysis of unreacted vinyl sulfone groups of HA2x hydrogels after 1 hour Michael addition cross-linking at 37°C. Comparison with standard vinyl sulfone and vinyl sulfone hydrolyzed from uncross-linked hydrogels (C).

Figure 2

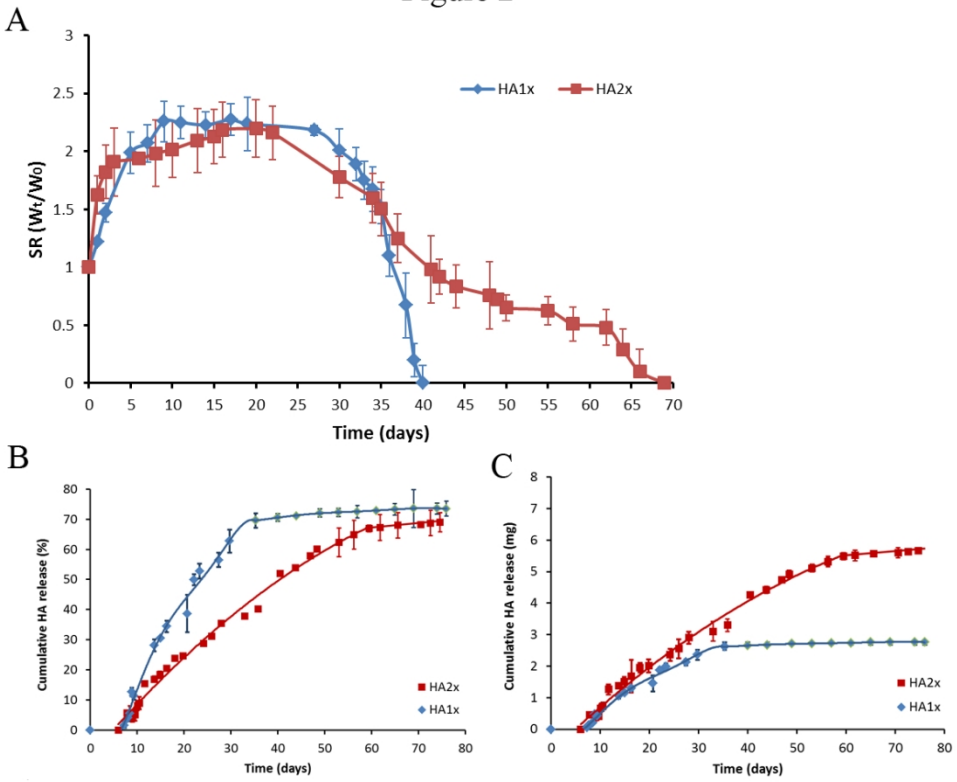

Figure 2. Swelling and degradation profiles of HA1x and HA2x hydrogels shown as the variation in time of the SR value during storage of the networks in physiological conditions (exposure to phosphate buffer at pH 7,4 and 37 °C (A). HA release profiles from HA1x and HA2x hydrogels: cumulative release profile % as a function of time (B); cumulative release profile in mg as a function of time (C).

Figure 3

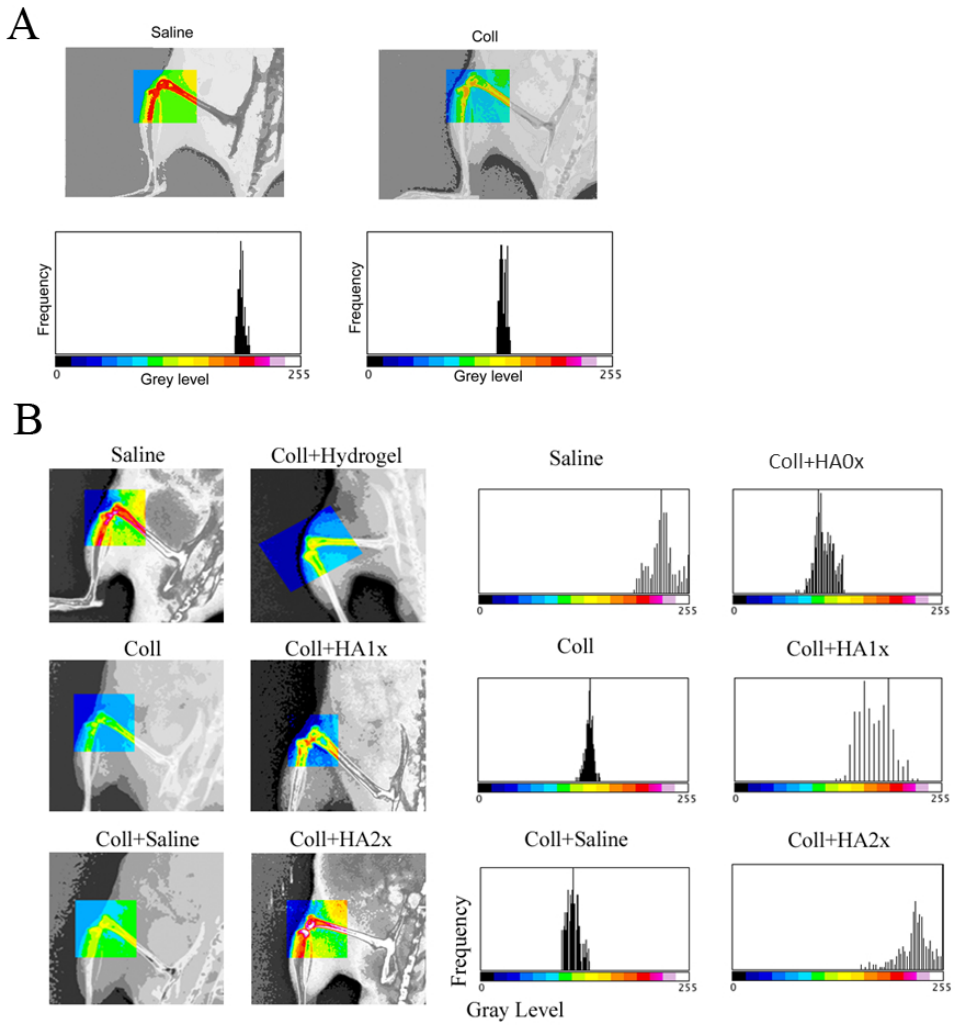

Figure 3. Pseudo-color images of X-ray images obtained converting the original 16 bit DICOM X-ray radiographs to an 8 bit TIFF format and pseudo-coloring the resultant image using a 16 color look-up table. In pseudo-color images, lower bone mineral density (BMD) is represented in green and yellow pseudo-colors, while higher BMD is represented in red and purple pseudo-colors. Histograms represent the BMD calculated in the areas selected (ROI). The decreased BMD after intraarticular injection of collagenase is visualized in green/yellow pseudo-color. The treatment with HA1A HA2x hydrogel in collagenase-injected mice resore the BMD, (yellow/purple and red/white pseudo-color, respectively) in dose dependent manner (A, B).

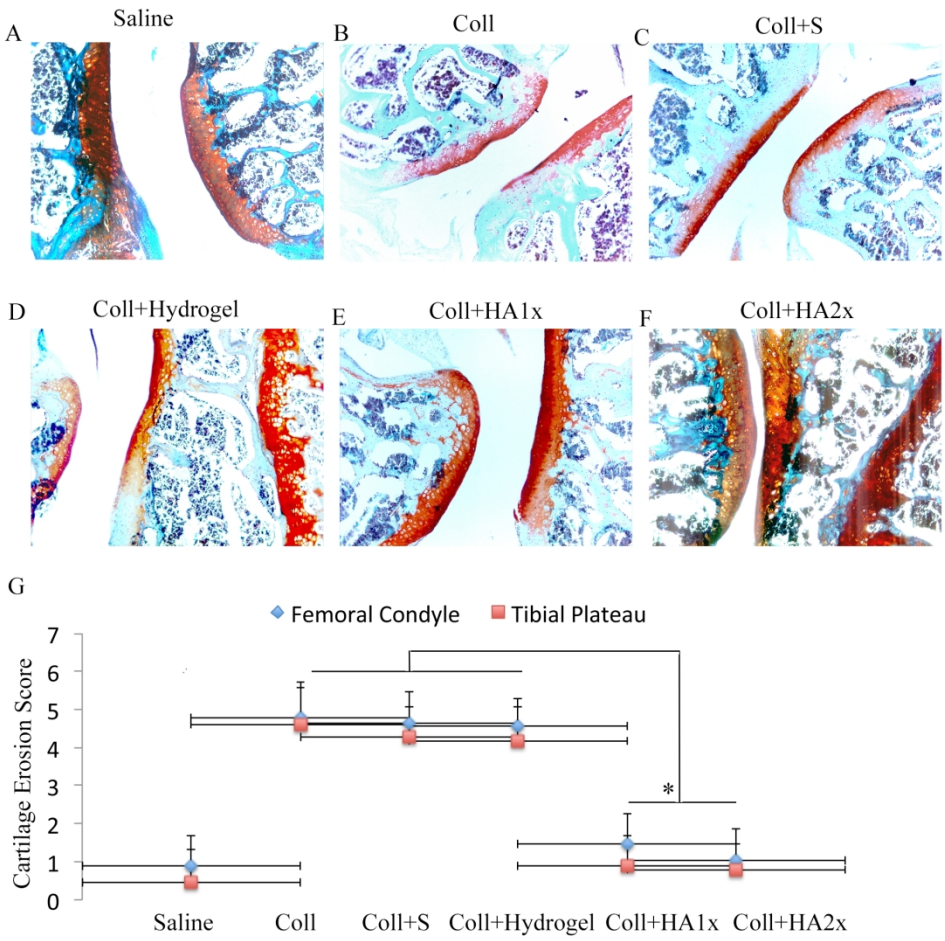

Figure 4. Representative Safranin-O/fast green stained histological sections of the knee joints in all mice groups (n = 6 mice/group) (A-F). Arrows indicated areas of hypocellularity after collagenase injection (B). HA1x and HA2x compounds reconstitute the cartilage thickness and cellularity (E, F). Magnification 10x. Cartilage erosion scores for femoral and tibial surfaces. Scores (mean±SE) shown with femoral condyles and tibial plateaus. Each group consisted of 6 animals (G).

Figure 5

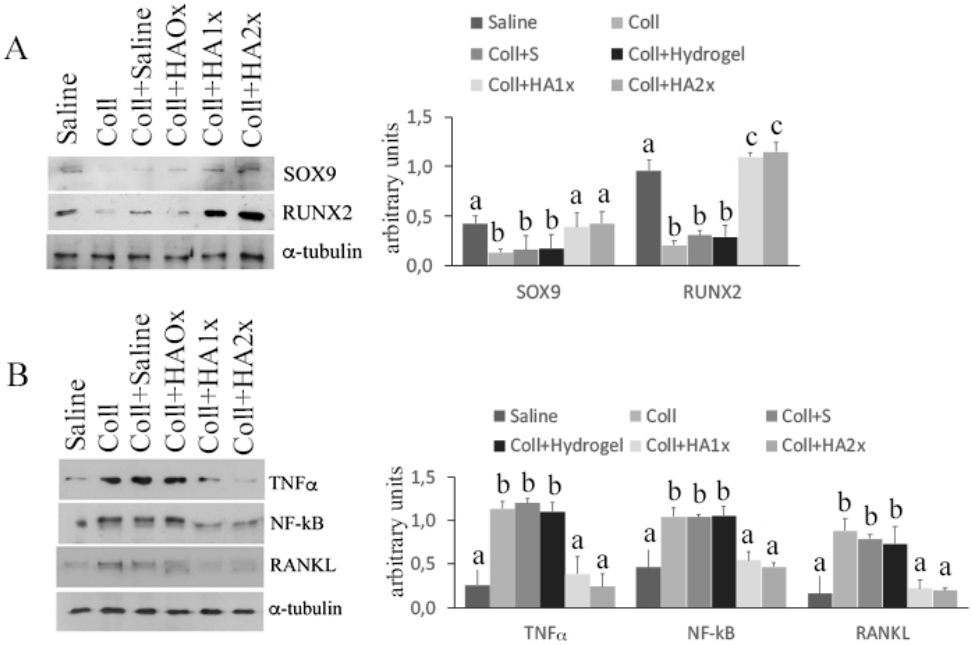

Figure 5. Representative western blotting of SOX-9 and RUNX2 expression levels in BMSCs obtained from all the mice groups (A). Representative western blotting of TNF-α, NFkB, and RANKL levels in BMSCs from all the mice groups (B). Data were analyzed by using two-way ANOVA. Lowercase letters denote homogeneous subsets. Error bars represent ± SE ($p < 0.05$)

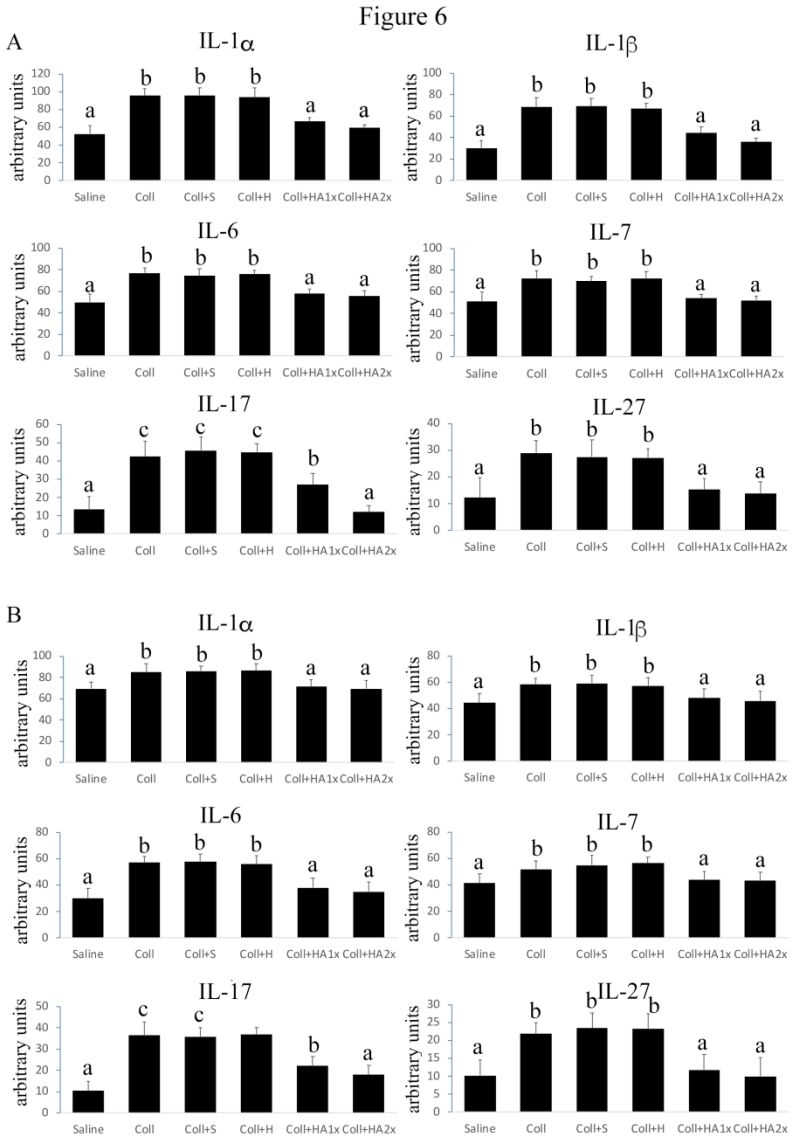

Figure 6. Cytokines release analyzed in medium from total bone marrow cell (BMCs) cultures (A) and in serum (B) of the all mice groups; Data were analyzed by using two-way ANOVA. Lowercase letters denote homogeneous subsets. Error bars represent ± SE ($p < 0.05$)

Table 1. Overview of the main characteristics of the polymers used in the formulation of the hydrogels studied in the present work.

	Mn* (kDa)	Mn** (kDa)	Mw** (kDa)	PDI**	Cloud point□ (°C)	DS* (%)	Yield (%)
VinylSulTC_0	47	25.7	52.5	2.04	24	0	70
VinylSulTC_10	54	25.8	54.2	2.1	22	8	100
VinylSulTC_15	55	26.1	57.2	2.06	19	16	97
HA-SH_56	38	-	37.9†	-	-	18	82

*Based on ^{1}H-NMR
**Based on GPC
□ Based on Light Scattering
† According to producer specifications

Table 2. Table summarizing mice groups use and treatments

GROUP	**Intraarticular injection**	**Intradermal Injection**	
G1 *(6 mice)* control	Saline 10 µl	No further treatment	
G2 *(30 mice)*	Collagenase 10 µl (1 mg/ml)	**G2a** *(6 mice)*	No further treatment
		G2b *(6 mice)*	50 µl saline
		G2c *(6 mice)*	50 µl hydrogel 15% w/w VinylSulfTC_0 (**HA0x**)
		G2d *(6 mice)*	50 µl hydrogel 15% w/w VinylSulfTC_10 4.1% w/w HA-SH_56 (**HA1x**)
		G2e *(6 mice)*	10 µl hydrogel 15% w/w VinylSulfTC_15 8.2% w/w HA-SH_56 (**HA2x**)